



A microfluidics-based stem cell model of early post-implantation human development

Yi Zheng¹, Yue Shao^{1,4} and Jianping Fu^{1,2,3}✉

Early post-implantation human embryonic development has been challenging to study due to both technical limitations and ethical restrictions. Proper modeling of the process is important for infertility and toxicology research. Here we provide details of the design and implementation of a microfluidic device that can be used to model human embryo development. The microfluidic human embryo model is established from human pluripotent stem cells (hPSCs), and the resulting structures exhibit molecular and cellular features resembling the progressive development of the early post-implantation human embryo. The compartmentalized configuration of the microfluidic device allows the formation of spherical hPSC clusters in prescribed locations in the device, enabling the two opposite regions of each hPSC cluster to be exposed to two different exogenous chemical environments. Under such asymmetrical chemical conditions, several early post-implantation human embryo developmental landmarks, including lumenogenesis of the epiblast and the resultant pro-amniotic cavity, formation of a bipolar embryonic sac, and specification of primordial germ cells and gastrulating cells (or mesendoderm cells), can be robustly recapitulated using the microfluidic device. The microfluidic human embryo model is compatible with high-throughput studies, live imaging, immunofluorescence staining, fluorescent in situ hybridization, and single-cell sequencing. This protocol takes ~5 d to complete, including microfluidic device fabrication (2 d), cell seeding (1 d), and progressive development of the microfluidic model until gastrulation-like events occur (1–2 d).

Introduction

The first few weeks of human embryo development after conception are crucial for successful pregnancy and fetus health^{1,2}. The pre-implantation development of the human embryo can be studied using surplus in vitro fertilization human embryos donated for research^{3–6}. However, the post-implantation development of the human embryo remains largely mysterious, due to technical difficulties and ethical constraints in obtaining post-implantation human embryo samples. Thus, the critical phase of human development from 7 d post-fertilization (when the human embryo implants into the uterus) to ~28 d post-fertilization (when it becomes possible to obtain embryonic tissues from abortion clinics) is often referred as the ‘black box’ of human development^{7–10}. During this period, while the human embryo establishes its connection to the maternal tissue, the pluripotent epiblast (EPI) undergoes morphogenetic events that give rise to a bipolar embryonic sac structure—an asymmetrically patterned epithelial tissue that encloses the pro-amniotic cavity, and through gastrulation, the three germ layers. So far, most of our knowledge on mammalian development has been obtained from studies of the mouse embryo. However, caution is required when extrapolating data from mice to humans due to the morphological and genetic differences between these two species^{11,12}. To address these limitations, significant progress has been achieved by prolonging in vitro culture of human and non-human primate (NHP) embryos toward the gastrulation stage^{13–17}. Although these embryo culture studies have facilitated understanding of the post-implantation primate embryo development, ethical restrictions and technological difficulties still prevent detailed mechanistic investigations using human and NHP embryos. In addition, insufficient human and NHP embryonic materials remain a significant limitation.

Human pluripotent stem cells (hPSCs) resemble the post-implantation, pre-gastrulation EPI in the human and NHP embryos in terms of molecular properties and lineage potency^{4,18,19}. Thus, hPSCs are considered to reside in a pluripotent state ‘primed’ for successive germ layer lineage commitment^{20,21}. hPSCs have been successfully utilized to develop human embryo models (or embryoids) for

¹Department of Mechanical Engineering, University of Michigan, Ann Arbor, MI, USA. ²Department of Cell and Developmental Biology, University of Michigan Medical School, Ann Arbor, MI, USA. ³Department of Biomedical Engineering, University of Michigan, Ann Arbor, MI, USA. ⁴Present address: Institute of Biomechanics and Medical Engineering, Department of Engineering Mechanics, School of Aerospace Engineering, Tsinghua University, Beijing, China. ✉e-mail: jpfu@umich.edu

modeling post-implantation human embryo development^{22–28}. However, most existing human embryoid systems either lack a resemblance to the 3D embryo architecture²² or rely on spontaneous organization and differentiation in uncontrolled environments without desired efficiency and reproducibility for mechanistic studies^{23,24,27,28}.

In this protocol, we describe in detail a microfluidic culture system that we previously developed and used to investigate early post-implantation human embryo development²⁹. This microfluidic human embryoid system enables the recapitulation of several key developmental landmarks of early post-implantation human embryo development, including the lumenogenesis of the EPI, formation of an asymmetrical embryonic sac, primordial germ cell (PGC) specification, and development of gastrulating cells (or mesendoderm cells) in the EPI with controlled anterior/posterior polarity²⁹.

Comparison with other human embryoid systems

Recently, several mouse embryoids have been successfully developed using different mouse stem cells (pluripotent stem cells, extended pluripotent stem cells, trophoblast stem cells, and extraembryonic endoderm stem cells) to model the pre- and post-implantation development of the mouse embryo^{30–37}. Compared with mouse embryoids, the development of human embryoids has so far been limited to primed hPSCs and thus to developmental events associated with the post-implantation human EPI; For example, human gastrulation embryoids have been developed by culturing primed hPSCs on 2D adhesive micropatterns of various sizes before treatments with exogenous bone morphogenetic protein (BMP)4 and/or Wnt signals^{22,38}. Previous studies showed that primed hPSCs have an intrinsic lumenogenic property and can spontaneously cluster and self-organize into spherical tissues containing a single central apical lumen^{23,39}. Importantly, when primed hPSCs are cultured in a 3D biomimetic native hydrogel environment ('Gel-3D'), some cells in each hPSC cluster spontaneously initiate amniogenic differentiation from focal regions of the cell cluster before amniogenic differentiation propagates to adjacent cells²³. Most of the hPSC clusters in Gel-3D gradually differentiate into uniform, squamous amniotic tissues within 5 d. In a subset of these hPSC clusters (<10%), however, distinct molecular and cellular asymmetries are evident, with squamous amniotic cells at one pole and columnar EPI-like cells at the opposite pole, reminiscent of the asymmetric embryonic sac in the early post-implantation human embryo²⁴. Progressive development of the asymmetric embryonic sac-like tissue in Gel-3D further exhibits features associated with the gastrulation in the columnar EPI-like compartment²⁴. Amniogenic differentiation of hPSCs in Gel-3D requires autonomous BMP-SMAD signaling, as blocking BMP signaling using Noggin or small-molecule drugs inhibits amniogenic differentiation of hPSCs in Gel-3D²³. Parametrical studies show a prominent effect of initial cell seeding density on the development of the asymmetric embryonic sac-like tissue in Gel-3D²³.

In another, more recently developed 3D human embryoid, pluripotent luminal epithelial tissues formed by primed hPSCs are treated with low doses of exogenous BMP4 to model the anterior–posterior symmetry breaking of the EPI at the onset of human gastrulation²⁷. In another set of human embryoids, 2D micropatterned hPSC colonies cultured under neural induction environments have been utilized for modeling the neurulation process^{25,26}. In 3D hydrogel environments, mouse PSCs and hPSCs cultured under a neurogenic condition followed by caudalization and/or ventralization self-organize and resolve into regionally patterned luminal neuroepithelial sacs, mimicking the development and regional patterning of the spinal cord^{28,40}.

The development of the asymmetric embryonic sac-like tissue in Gel-3D remains the only human embryoid system that can successively recapitulate landmarks of the development of the EPI and amniotic ectoderm (AM) parts of the early post-implantation human embryo. The development of the asymmetric embryonic sac-like tissue in Gel-3D, like many other 3D organoid cultures, however, is of low efficiency, preventing its use as a tractable experimental system for detailed mechanistic investigations. To address this critical issue, we recently developed a microfluidic human embryoid system with significantly improved controllability and efficiency, thus rendering the microfluidic human embryoid system a tractable experimental platform to study previously inaccessible phases of early post-implantation human development.

Using microfluidics to study human embryoid development

The development of the asymmetric embryonic sac-like tissue in Gel-3D is of low efficiency, preventing clear understanding of the molecular and cellular asymmetries and the formation of the amniotic–embryonic axis. Thus, we recently sought to leverage microfluidics and its superior control of dynamic cell culture environments in miniaturized channels to generate human embryoids in a

controllable and scalable manner. Microfluidics allows precise control of the location and initial cell number of individual cell clusters, some key requirements for improving the controllability of human embryoid development. Furthermore, microfluidics can be conveniently applied to generate dynamic and graded morphogen signals, which is a powerful feature to control patterning and multicellular self-organization^{41,42}. Importantly, microfluidic devices are often compatible with live imaging and standard biochemical assays, such as immunofluorescence staining and fluorescent *in situ* hybridization (FISH), and can be integrated with microfabricated cell mechanics tools^{43,44}, promoting quantitative measurements and perturbations of both biochemical and biomechanical signals down to a resolution that is not possible with conventional embryology studies.

Design of our microfluidic human embryoid system

Figure 1 shows the design of the microfluidic device and the procedure to generate an array of hPSC clusters in prescribed locations in the device. Specifically, the microfluidic device contains three parallel channels partitioned by evenly spaced, trapezoid-shaped supporting posts, with the central channel (gel channel) preloaded with native hydrogel Geltrex. Geltrex contraction during gelation leads to formation of concave gel pockets between adjacent supporting posts. One of the other two outside channels is labeled as the cell-loading channel, into which hPSCs are injected. The opposite channel is labeled as the induction channel (Fig. 1a). After hPSC cluster formation, different exogenous factors can be introduced into either or both of the cell-loading and induction channels to model specific early post-implantation human embryonic developmental processes.

The dimension of the microfluidic device is shown in Fig. 1b. In its current design (computer-aided design (CAD) and pdf files available in Supplementary Data), each microfluidic device can generate an array of 17 hPSC clusters. The dimension of the microfluidic device needs to be optimized for specific experimental purposes. To improve the throughput of toxicological screening, the system can be conveniently scaled up by increasing the channel length to contain more clusters. We anticipate that no significant modification of the procedure would be needed for generating up to 100 clusters per device. Key parameters include the distance between adjacent supporting posts, the geometry of the supporting post, and the thickness of the microfluidic channel. The gap distance between adjacent supporting posts directly determines the hPSC cluster size and the number of hPSCs within each gel pocket. A gap distance of 60–100 μm between adjacent supporting posts has been successfully tested using the procedure we describe here. The trapezoid shape of the supporting posts is optimal for confining Geltrex within the gel channel by surface tension, the angles of which should not be changed significantly, while the parallel sides of the supporting posts can be adjusted to control how far apart adjacent hPSC clusters are. The thickness of the microchannel also affects the gel pocket size and is recommended to be the same as the gap distance between adjacent supporting posts.

The gap distance between adjacent supporting posts and their geometry are determined when designing the CAD file of the photomask used for the microfabrication of the microfluidic device. The thickness of the microchannel is controlled during the microfabrication process.

We have successfully used this protocol on both human embryonic stem cells (hESCs; H1 and H9) and induced pluripotent stem cells (hiPSCs; 1196a), maintained in either mTeSR1 or Essential 8. The protocol reported here has been optimized to tolerate possible variations caused by different hPSC lines and medium conditions used for their culture. The results generated using the above-mentioned cells and medium conditions are quite consistent, except that the clusters of cells maintained in mTeSR1 are rounder compared with when using Essential 8. To best repeat the protocol reported here, we recommend that all the instructions in each step be followed. If needed, possible variations/optimizations are also included in corresponding steps of the 'Procedure' section. We have found that, when the protocol is carried out properly, it is highly reproducible and over 90% of the cell clusters will develop into asymmetric embryonic sac-like tissue, leading to consistent results across different devices and independent experiments²⁹. To obtain statistically meaningful results, we find that three or four devices are sufficient per condition for each experiment.

Applications and limitations of the microfluidic human embryoid system

This system was deliberately engineered to avoid modeling the complete human embryo. The embryonic sac-like tissues generated in this protocol lack the primitive endoderm and the trophoblast, and thus cannot form a yolk sac or placenta, respectively. The incompleteness of this reported model is advantageous from an ethical standpoint, which significantly alleviates the ethical concerns

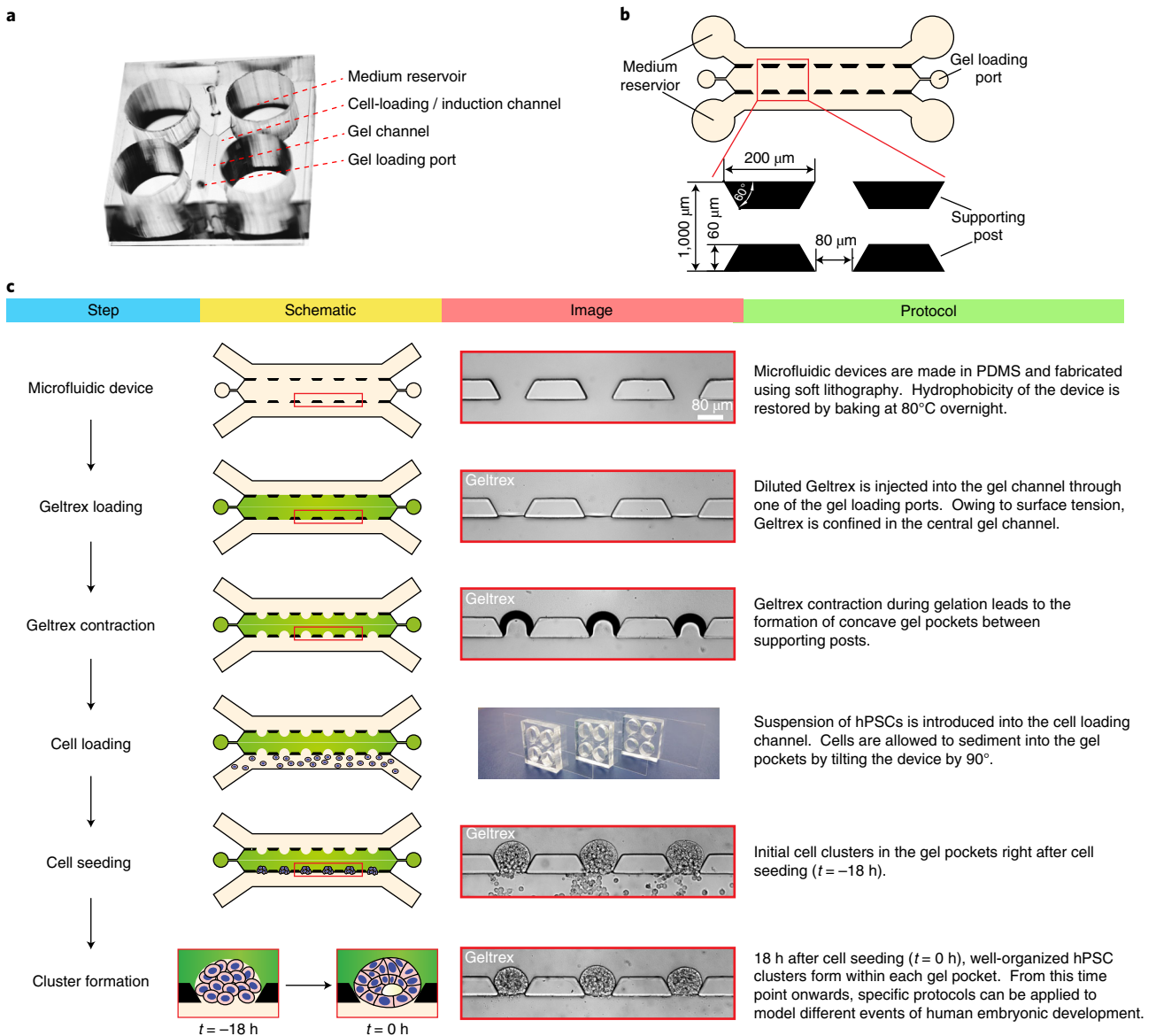


Fig. 1 | Design and preparation of the microfluidic device and scheme of cell loading to establish initial cell clusters. **a**, Photograph showing the microfluidic device. Medium reservoirs, gel-loading ports, and cell-loading and induction channels are indicated. **b**, Design of the microfluidic device incorporating three parallel channels (80 μm in height) partitioned by trapezoid-shaped supporting posts spaced 80 μm apart. The central gel channel is preloaded with Geltrex basement membrane matrix. The other two, outside channels are used for cell loading (the cell-loading channel) and chemical induction (the induction channel), respectively. **c**, Schematic diagrams and photographs showing experimental steps to establish initial clusters of hPSCs. Note that the protocol is optimized for hPSCs maintained in mTeSR1 and the microfluidic device with dimensions indicated in **b**. **b** and **c** are adapted from ref. ²⁹.

regarding and restrictions on research on human embryos. Specifically, in the microfluidic device, dissociated single hPSCs loaded into the cell-loading channel are guided to form a regular array of spherical hPSC clusters in prescribed locations. These hPSC clusters soon spontaneously undergo lumenogenesis and form a single central lumen, mimicking the formation of the pro-amniotic cavity enclosed by the EPI upon implantation of the human embryo. The compartmentalized configuration of the microfluidic device allows two opposite regions of each hPSC cluster to be exposed to different exogenous chemical environments. Using the microfluidic device, we generated asymmetric embryonic sac-like tissues with an efficiency of ~95%, which is greater than that reported using Gel-3D²⁹. Importantly, the microfluidic human embryoid system enables the recapitulation of successive key early human post-implantation developmental landmarks in a highly controllable and scalable fashion, including the lumenogenesis of the EPI, formation of the bipolar embryonic sac, specification of PGCs, and development of gastrulating cells (or mesendoderm cells) in the EPI with

Box 1 | Live cell imaging

The microfluidic device is compatible with live cell imaging. Special care needs to be taken to mitigate medium evaporation from the medium reservoirs of the microfluidic device, as described below.

Procedure

- 1 Use a smaller coverslip, for example, 22 mm × 22 mm, for fabrication of the microfluidic device (Step 5).
- 2 At $t = 0$ h, place the microfluidic device in a 35-mm Petri dish with a 13-mm hole at the dish bottom (Step 22).
- 3 Use Scotch tape to secure the microfluidic device in the dish and seal the hole at the dish bottom (at Step 22).
- 4 Place some wet tissue papers and add sterile distilled water into the Petri dish (at Step 22).
▲ CRITICAL STEP Make sure the water does not come into contact with the medium reservoirs.
- 5 Close the lid of the Petri dish, and then mount the dish on an inverted epi-fluorescence microscope for live cell imaging (from Step 22 onward). There is no need to add or exchange medium for 48 h, if the environmental chamber enclosing the microscope is humidified.

controlled anterior/posterior polarity²⁹. It is also worth noting that this microfluidic human embryoid system can be conveniently adopted by cell biology laboratories, since it does not require fluid handling equipment such as tubing, syringe pumps, or valves, which are commonly needed for more sophisticated microfluidic devices^{45,46}.

The microfluidic human embryoid system is compatible with live imaging (if the procedure is modified as described in Box 1), immunofluorescence staining (as described in Step 23B), and FISH and single-cell sequencing (the dissociation of single cells is described in Step 23A). Given its controllability and reproducibility, it can be utilized, in conjunction with genetically modified hPSC lines, to conduct quantitative assays to study fundamental questions in human development, including the molecular basis of amniogenesis, the symmetry breaking and patterning of the bipolar embryonic sac, the origin and specification of PGCs, the role of AM in the epithelial–mesenchymal transition of the EPI, and the molecular and cellular mechanisms underlying germ layer lineage allocation during gastrulation. Given that the goal of driving differentiation of hPSCs toward therapeutically relevant cell lineages requires cells to pass through the bottleneck of germ layer specification efficiently *in vitro* before further specialization, it is of utmost importance to improve our knowledge of human gastrulation for stem-cell-based cell therapies and regenerative medicine.

The microfluidic human embryoid system can only be cultured for ~4–5 d. This short window of culture time is due to the limited space within the microfluidic device, constraining the continuous growth and development of the human embryoid. Furthermore, disseminating cells from the human embryoid mimicking gastrulation and mesendoderm induction lead to collapse and disassembly of the human embryoid structure. It should also be noted that the EPI-like compartment of the microfluidic human embryoid can only be either posteriorized or anteriorized and thus lacks an anterior–posterior axis. Future efforts could be devoted to identifying a strategy to prolong the culture time of the human embryoid and promote self-organization of gastrulating cells to mimic the emergent trilaminar germ disk formation in the human embryo. As shown in mouse embryoids, the crosstalk between embryonic and extraembryonic compartments is critical for promoting the proper organization and continuous development of embryoids^{30–37}. It is possible that adding human hypoblast stem cells, which have become available very recently and may still require additional authentication^{47,48}, to the microfluidic human embryoid could be helpful for these efforts.

Further experimental design details

The microfluidic device is made of polydimethylsiloxane (PDMS), and soft lithography is required to fabricate the PDMS microfluidic device (Fig. 1a). Prior to this, a silicon or SU-8 mold must be fabricated using standard microfabrication, which requires access to a cleanroom facility, or can be outsourced. This is described briefly in the reagent setup section, with further details available elsewhere^{49–51}. Once the silicon or SU-8 mold is fabricated, if handled carefully, it can be reused for a long period of time (many years). The structural parameters of the microfluidic device can be adjusted to accommodate different experimental requirements; we provide the CAD file we use to create an array of 17 hPSC clusters with a 80- μ m gap distance between adjacent supporting posts in Supplementary Data. All other equipment and reagents required are commercially available.

Materials

Biological materials

We have successfully used this protocol starting from both hESCs and hiPSCs, as discussed in the Introduction. Lines that have been used successfully include H9 (WA09, WiCell; NIH registration no. 0062; RRID: [CVCL_9773](#)), H1 (WA01, WiCell; NIH registration no. 0043; RRID: [CVCL_9771](#)), and 1196a (a hiPSC line from the University of Michigan Pluripotent Stem Cell Core⁵²; RRID: [CVCL_ZJ39](#)). We did not observe significantly different success rates or developmental timing among the above-mentioned stem cell lines²⁹ **! CAUTION** Any experimental protocol using hPSCs must comply with national and regional laws and institutional ethical guidelines and regulations^{53,54}. We obtained permission from the Human Pluripotent Stem Cell Research Oversight Committee at the University of Michigan, Ann Arbor to undertake the experiments from which we show results here. **▲ CRITICAL** hPSCs should be regularly authenticated and checked for mycoplasma contamination.

Reagents

- A positive silicon mold made using deep reactive ion etching (DRIE)
- PDMS (Dow SYLGARD 184)
- Coverslip (Electron Microscopy Sciences, cat. no. 72210-20)
- DMEM/F12 (Gibco, cat. no. 11330-033)
- mTeSR1 (STEMCELL Technologies, cat. no. 85850)
- Geltrex basement membrane matrix (Thermo Fisher Scientific, cat. no. A1413202)
- ROCK inhibitor Y27632 (Tocris, cat. no. 1254)
- Dispase (Gibco, cat. no. 17105-041)
- Accutase (Sigma-Aldrich, cat. no. A6964)
- Essential 6 medium (Thermo Fisher Scientific, cat. no. A1516401)
- Essential 8 medium (STEMCELL Technologies, cat. no. 05990)
- FGF-Basic (AA 1–155; Thermo Fisher Scientific, cat. no. PHG0266)
- BMP4 (R&D Systems, cat. no. 314-BP-050)
- Activin (R&D Systems, cat. no. 338-AC-050)
- Noggin (R&D Systems, cat. no. 6057-NG-025)
- IWP2 (Tocris, cat. no. 3533)
- Dimethyl sulfoxide (DMSO; Sigma-Aldrich, cat. no. D2650-100ML)
- PBS (Gibco, cat. no. 10010-023)
- Sodium dodecyl sulfate (SDS; Sigma-Aldrich, cat. no. 436143-25G)
- NaN₃ (VWR, cat. no. BDH7465-2) **! CAUTION** Toxic. Chemical hood, protective clothing, gloves, and glasses are needed. Comply with national and regional regulations for hazardous waste disposal.
- Donkey serum (Sigma-Aldrich, cat. no. D9663-10ML)
- Paraformaldehyde (PFA; Electron Microscopy Sciences, cat. no. 15710) **! CAUTION** Toxic. Chemical hood, protective clothing, gloves, and glasses are needed. Comply with national and regional regulations for hazardous waste disposal.
- DAPI (Thermo Fisher Scientific, cat. no. D1306)
- Wheat germ agglutinin (WGA; Thermo Fisher Scientific, cat. no. W21404)
- Antibodies (Table 1)

Equipment

- CO₂ incubator (Thermo Fisher Scientific, cat. no. Heracell 150i)
- Biological safety cabinet (Labconco, cat. no. 3460001)
- Glass hemocytometer (Hausser Scientific, cat. no. 1475)
- Desiccator (Bel-Art, cat. no. F42025-0000)
- Hotplate (Fisher Scientific, cat. no. 11-102-49SH)
- Biopsy punch (Ted Pella, cat. no. 15111-80)
- Harris Uni-Core punch (GE Healthcare, cat. no. WB100028)
- Adhesive tape (Scotch tape, 3M Science. Applied to Life, model: Scotch Magic Greener Tape)
- Ultrasonic cleaner (Branson, cat. no. 1510)
- Oxygen plasma machine (FEMTO SCIENCE, model: COVANCE-1MP)
- Oven (110 °C; Fisher Scientific, model: Isotemp 625G gravity oven)
- Oven (80 °C; Cole-Parmer, model: StableTemp digital mechanical convection oven)
- Scale (Denver Instrument, cat. no. S-402)

Table 1 | Antibodies

	Vender and catalog number	Research resource identifiers (RRIDs)	Species	Dilution
Primary antibodies				
EZRIN	Sigma-Aldrich, cat. no. E8897	AB_476955	Mouse	1:2,000
OCT4	Santa Cruz Biotechnology, cat. no. sc-5279	AB_628051	Mouse	1:200
OCT4	Cell Signaling Technology, cat. no. 2750	AB_823583	Rabbit	1:500
NANOG	Cell Signaling Technology, cat. no. 4903	AB_10559205	Rabbit	1:500
SOX2	Stemgent, cat. no. 09-0024	AB_2195775	Rabbit	1:500
TFAP2A	Santa Cruz Biotechnology, cat. no. sc-12726	AB_667767	Mouse	1:100
TFAP2C	Santa Cruz Biotechnology, cat. no. sc-12762	AB_667770	Mouse	1:100
BRACHYURY	Thermo Fisher Scientific, cat. no. PA5-46984	AB_2610378	Goat	1:100
SOX17	R and D Systems, cat. no. AF1924	AB_355060	Goat	1:500
CDX2	BioGenex, cat. no. AM392	AB_2650531	Mouse	1:300
FOXA2	Cell Signaling Technology, cat. no. 8186	AB_10891055	Rabbit	1:300
EOMES	Abcam, cat. no. ab23345	AB_778267	Rabbit	1:200
Secondary antibodies				
Anti-Rabbit 546	Thermo Fisher Scientific, cat. no. A-10040	AB_2534016	Donkey	1:500
Anti-Mouse 488	Thermo Fisher Scientific, cat. no. A-21202	AB_141607	Donkey	1:500
Anti-Goat 647	Thermo Fisher Scientific, cat. no. A-21447	AB_2535864	Donkey	1:500

- Centrifuge (Eppendorf, cat. no. 5702)
- Inverted microscope (Carl Zeiss MicroImaging, model: Zeiss Observer.Z1)
- Confocal microscope (Olympus, model: DSUIX81)
- Nunc cell-culture-treated six-well plates (Thermo Fisher Scientific, cat. no. 140675)
- Petri dishes (Fisher Scientific, cat. nos. FB0875714 and FB012920)
- 35-mm Petri dish with 13-mm hole (Cell E&G, cat. no. PDH00001-200)
- Pipettes (Eppendorf, P1000, P200, and P20)
- Stereomicroscope (We use Zeiss, model: Invertoskop 40C)
- Water bath (Thermo Fisher Scientific, cat. no. 2845)
- Pasteur pipette rubber bulb (Sigma-Aldrich, cat. no. Z111597-12EA)
- Cell scraper (Fisher Scientific, cat. no. 08-100-240)
- Common consumables (serological pipettes, centrifuge tubes, pipette tips, and blades)

Reagent setup

Stock solutions

Stock solutions of all the proteins and chemicals listed in 'Reagents' should be prepared and stored following manufacturers' instructions. Use PBS as the buffer when preparing a working solution of SDS. The working solution can be stored at room temperature (20–25 °C) for a year (protect from light). Use PBS as the buffer when preparing working solution of PFA. The working solution can be stored at room temperature for a year (protect from light).

Dispase

Prepare a 2 mg mL⁻¹ solution of Dispase with DMEM/F12, and store at –20 °C for up to 2 years. Add DMEM/F12 to a working concentration of 0.2 mg mL⁻¹, and store at 4 °C for up to 1 month.

Feeder-free culture of hPSCs

This protocol works for hPSCs maintained in mTeSR1 or E8 medium. To achieve the best results, we suggest maintaining hPSCs on Geltrex-coated tissue culture plates using mTeSR1. Briefly, six-well tissue culture plates are coated with 1% (vol/vol) Geltrex for 1 h in a CO₂ incubator (37 °C, 5% CO₂). Feeder-free hPSCs are passaged using 0.2 mg mL⁻¹ Dispase diluted in DMEM/F12. Detailed protocols for feeder-free culture of hPSCs using mTeSR1 or E8 medium can be found in the manufacturer's instructions.

Geltrex aliquots

Thaw Geltrex (5 mL vial) on ice in a 4 °C fridge overnight and mix well before dividing into small aliquots (150–200 µL) under sterile conditions. Keep a record of the lot number and protein concentration listed on the product specification sheet. Store aliquots at –20 or –80 °C for up to 2 years. Thaw for 2–3 h on ice in a 4 °C fridge before use. **▲ CRITICAL** During experiments, Geltrex should be kept constantly on ice. Solidification of Geltrex will severely affect the Geltrex loading process and formation of the concave Geltrex pocket.

Basal medium

Essential 6 medium containing FGF2 (20 ng mL⁻¹) is used as a basal medium (BM). **▲ CRITICAL** Make up BM fresh before each use.

Microfluidic device mold fabrication

Fabricate the silicon mold using the standard DRIE method. The operational conditions for DRIE (for example, temperature, gas flows, pressure, and radiofrequency power) strongly depend on the specific equipment used. Therefore, it is necessary to consult with the cleanroom technicians to obtain detailed instructions for the specific DRIE equipment available before usage. Example microfabrication workflows can be found in refs. ^{49,50}. Alternatively, if DRIE equipment is not available, the mold can also be fabricated using standard soft lithography methods with SU-8. Instrument setups and detailed procedures for soft lithography using SU-8 can vary by facility. A general guideline is available elsewhere⁵¹. AutoDesk AutoCAD is recommended for photomask design to determine the geometry of the mold. The CAD file used for this protocol is included in the Supplementary Data. Alternatively, fabrication of the microfluidic device mold can be outsourced to external facilities by providing the CAD file.

Blocking solution (for immunofluorescence only)

PBS containing 4% (vol/vol) donkey serum and 0.1% (wt/vol) NaN₃ is used as blocking solution for immunofluorescence. The blocking solution can be stored in a 4 °C fridge for a month.

Procedure**Microfluidic device fabrication ● Timing -2 d**

▲ CRITICAL This section requires the silicon wafer positive mold which has been fabricated already using the standard DRIE method as described in 'Reagent setup' section. The design of the microfluidic device incorporates three parallel channels (80 µm in height) partitioned by trapezoid-shaped supporting posts spaced 80 µm apart (Fig. 1b). The design of the device (CAD file) is included in the Supplementary Data.

- 1 Mix PDMS curing agent and pre-polymer thoroughly at 1:10 weight ratio, and degas the mixture in a desiccator for 40 min.
- 2 Cast PDMS mixture onto the silicon mold, and bake at 110 °C for 60 min in a convection oven. After baking, peel the PDMS layer off the silicon mold.
■ PAUSE POINT After cooling down, the PDMS layer can be stored in a clean Ziploc bag at room temperature for a few months.
- 3 Punch medium reservoirs (8 mm in diameter) using biopsy punch tools and gel-loading ports (1.2 mm in diameter) using Harris Uni-Core punch tools at appropriate locations of the PDMS layer (see Fig. 1a for guidance regarding where to punch the holes). Cut the PDMS layer into individual devices using blades.
- 4 Clean PDMS using adhesive tape to remove particles and debris.
- 5 Wash coverslips with ethanol in an ultrasonic cleaner for 15 min before drying with pressurized air.
- 6 Bake coverslips at 110 °C in a convection oven for 20 min.
- 7 Treat PDMS and coverslips with oxygen plasma for 30 s. Bond PDMS and coverslip by slightly applying pressure for 30 s on a 120 °C hotplate, then bake in an 80 °C convection oven overnight.
▲ CRITICAL STEP The power and duration of oxygen plasma treatment should be optimized based on the specific instruments used. Imperfect bonding can lead to leakage during experiments. Bonding quality can be visually inspected using a microscope. Baking at 80 °C overnight is required to restore the hydrophobicity of the PDMS device, which is critical for the following gel-loading step.

? TROUBLESHOOTING

Geltrex injection ● Timing ~1 d

- 8 Expose the PDMS device to UV light for 30 min in a biological safety cabinet.
- 9 Prepare a humidified chamber by putting a 35-mm Petri dish filled with sterile DI water into a 150-mm Petri dish. Place the humidified chamber in a CO₂ incubator (37 °C, 5% CO₂). This humidified chamber is to prevent medium evaporation from the microfluidic device.
- 10 Dilute Geltrex with cold E6 medium to achieve a final protein concentration of 8–11 mg mL⁻¹. The Geltrex concentration needs to be optimized for different Geltrex lots.
▲ CRITICAL STEP Keep Geltrex on ice all the time, and use cold (0–4 °C) E6 medium. Geltrex is very sensitive to temperature, and partially solidified Geltrex will result in experimental failure.
- 11 Inject diluted Geltrex into one of the gel-loading ports to fill the central gel channel using a pipette tip (Fig. 1c, geltrex loading step). The actual volume of Geltrex required to fill the gel-loading channel is very small, so we recommend using a 20-μL pipette tip and a minimum of 5 μL Geltrex.
▲ CRITICAL STEP Gel injection should be conducted very gently, so that the Geltrex can be confined in the central gel channel by surface tension. Geltrex does not need to fill the other gel-loading port.
? TROUBLESHOOTING
- 12 Place the microfluidic device in the humidified chamber in a CO₂ incubator (37 °C, 5% CO₂) for up to 10 min to allow Geltrex to solidify. While Geltrex solidifies, it forms concave gel pockets between supporting posts in the microfluidic device (Fig. 1c, geltrex contraction step).
▲ CRITICAL STEP Given lot-to-lot variation of Geltrex and the sensitivity of Geltrex solidification to environmental factors, check the gel pocket formation every 1–2 min after 5 min of incubation.
? TROUBLESHOOTING
- 13 When gel pockets reach a desired size (100–120 μm in diameter), add 140 μL mTeSR1 medium immediately to one reservoir of the induction channel. Gently apply vacuum to the other reservoir with a rubber dropper bulb to help fill the induction channel, then add 140 μL mTeSR1 medium to the other reservoir of the induction channel. Add 180 μL mTeSR1 medium to one reservoir of the cell-loading channel, and apply vacuum to the other reservoir with a rubber dropper bulb to help fill the cell-loading channel, then add 180 μL mTeSR1 medium to the other reservoir of the cell-loading channel.
▲ CRITICAL STEP A vacuum is required when filling the channels due to the hydrophobicity of the PDMS device. The pressure of the cell-loading channel needs to be higher than the induction channel, in order to maintain the gel pocket size.
- 14 Place the humidified chamber containing the microfluidic device in a CO₂ incubator (37 °C, 5% CO₂) for 18–24 h to stabilize the Geltrex structure and remove trapped air bubbles.

Cell seeding ● Timing 2–3 h

- 15 Take a plate of hPSC, remove mTeSR1, and rinse hPSC colonies twice with 1 mL DMEM/F12.
▲ CRITICAL STEP hPSCs need to have been appropriately maintained on Geltrex-coated tissue culture plates prior to this step. hPSC colonies should not show noticeable cell death at the colony center. No spontaneous differentiation of hPSCs should be noticeable on the tissue culture plate.
- 16 Dissociate hPSCs into single cells by incubation with Accutase at 37 °C for 7–10 min. Centrifuge the hPSC suspension at 200g at room temperature for 5 min, then resuspend hPSCs in mTeSR1 containing 10 μM Y27632 at concentration of 8 × 10⁶ cells mL⁻¹. Place cell suspension on ice while you proceed with the next step.
- 17 Empty all the reservoirs of the microfluidic device using a vacuum aspirator.
▲ CRITICAL STEP Empty only the reservoir wells but not the microfluidic channels by placing the tip of the vacuum aspirator away from the microfluidic channel inlets, and make sure the reservoirs are completely empty.
- 18 Introduce singly dissociated hPSCs into the cell-loading channel by pipetting 10 μL hPSC suspension at the inlet of the cell-loading channel. Allow single hPSCs to sediment into the gel pockets by tilting the microfluidic device by 90° for 10 min. After 5 min, gently pipette the 10 μL hPSC suspension in the medium reservoir to minimize cell aggregation in the reservoir (Fig. 1c, cell-loading step).
▲ CRITICAL STEP If the initial hPSC cluster in each gel pocket is too small, this step can be repeated. Note that the diameter of hPSC clusters at Step 22 (which is designated as *t* = 0 h) should be between 85 and 125 μm.
? TROUBLESHOOTING

Table 2 | Morphogens and antagonists required to model particular aspects of human embryonic development at Step 22

Targeted developmental process	Induction channel	Cell-loading channel
Epiblast-like cysts	Basal medium (BM)	BM
Posteriorized embryonic-like sacs (P-ELS)	BM + BMP4 (50 ng mL ⁻¹)	BM
Anteriorized embryonic-like sacs (A-ELS)	BM + BMP4 (50 ng mL ⁻¹)	BM + Noggin (50 ng mL ⁻¹) + IWP2 (5 μM in DMSO)
Posteriorized gastrulating cells	BM	BM + BMP4 (50 ng mL ⁻¹)
Anteriorized gastrulating cells	BM + Activin A (50 ng mL ⁻¹)	BM + BMP4 (50 ng mL ⁻¹)

- 19 Refill the medium reservoirs of the microfluidic device with mTeSR1 containing 10 μM Y27632. Add 200 μL per reservoir for the cell-loading channel and 50 μL per reservoir for the induction channel.
 - 20 Incubate the microfluidic device in a CO₂ incubator (37 °C, 5% CO₂) for 1–2 h.
- ? TROUBLESHOOTING**
- 21 Add 110 μL mTeSR1 containing 10 μM Y27632 to each medium reservoir of the induction channel (Fig. 1c, cell seeding step) and incubate for a further 18 h.

Microfluidic human embryoid generation ● Timing 1–2 d

- 22 Check that the hPSCs in the gel pocket have formed a cluster and initiated lumenogenesis (Fig. 1c, cluster formation step).
From this time point ($t = 0$ h) onward, coax clusters of hPSCs to model particular aspects of human embryonic development by introducing morphogens and/or antagonists via the cell-loading and/or induction channels (from $t = 0$ onward), as detailed in Table 2.

? TROUBLESHOOTING

▲ CRITICAL STEP The pressure of the induction channel needs to be higher than that of the cell-loading channel, to ensure that hPSC clusters entrapped in each gel pocket are pressed against supporting posts. We therefore recommend that 200 μL per reservoir be used for the cell-loading channel and 240 μL per reservoir for the induction channel. If the entire protocol takes less than 48 h, it is not usually necessary to replenish medium in the medium reservoirs.

Downstream analysis

- 23 At this stage in the procedure, there are various ways in which you can proceed. If you wish to dissociate the embryonic sac-like tissue into single cells to take samples at various time points, follow option A (e.g., for single-cell RNA sequencing). If you wish to fix and stain cells for immunofluorescent analysis at the end point of the assay, follow option B.

? TROUBLESHOOTING

(A) Retrieving cells for single-cell analysis ● Timing 2–3 h

▲ CRITICAL Since each device contains only ~5,000–10,000 cells, depending on the specific protocols and culture time, extra care should be taken when collecting medium containing dissociated single cells to avoid cell loss or damage. To obtain a sufficient number of singly dissociated cells, cells from multiple microfluidic devices can be pooled together. If 10× Genomics is used for single-cell RNA sequencing, we recommend pooling cells from six to nine devices to target the retrieval of 6,000–10,000 cells, and a minimum of 1,000 cells is needed for clustering all the main cell lineages in the microfluidic human embryoid.

- (i) Prepare PBSA solution (2% BSA in PBS, wt/vol) 1 d in advance. Filter PBSA solution to remove undissolved debris.
- (ii) Coat 1.5-mL microcentrifuge tube with PBSA for 1 h at room temperature.
- (iii) Carefully scratch the medium reservoirs of the cell-loading channel using a pipette tip. Agitate and then thoroughly aspirate medium to remove cells and debris from the medium reservoirs.
- (iv) Rinse the cell-loading channel and induction channel twice by adding 150–200 μL DMEM/F12 to each medium reservoir for 10 min each.

- (v) Add 80 μL Accutase to one reservoir of the cell-loading channel, and another 20 μL Accutase to one reservoir of the induction channel. Incubate the microfluidic device for 60 min in a CO_2 incubator (37 $^\circ\text{C}$, 5% CO_2).
▲ CRITICAL STEP Use a humidified chamber as described in Step 9. Prolong incubation time if necessary to ensure complete cell dissociation. The progress of cell dissociation in the microfluidic device can be checked under an inverted tissue culture microscope.
- (vi) Gently agitate the Accutase solution, and visually confirm the complete cell dissociation. Carefully collect Accutase solution containing dissociated single cells from all medium reservoirs in which cells have been dissociated and transfer into a 1.5-mL microcentrifuge tube on ice.
- (vii) Add PBSA until the 1.5-mL microcentrifuge tube is full. Place the microcentrifuge tube on ice for a further 10 min. Gently pipette every 5 min.
- (viii) Centrifuge at 300*g* for 5 min at 4 $^\circ\text{C}$. Check cell pellet formation by eye, and mark its position.
- (ix) Wash the cell pellet by first removing the supernatant, and then repeating Step 23A(vii and viii).
- (x) Remove supernatant until a desired volume is achieved.
- (xi) Proceed to single-cell RNA sequencing. We use 10 \times Genomics as described in ref. ²⁹ and recommend the use of the Seurat R package for single-cell RNA sequencing data analysis, as described in refs. ^{55,56}.

(B) Immunofluorescence staining ● Timing 2–3 d

- ▲ CRITICAL** In all the following steps, be careful when aspirating solutions from the medium reservoirs to only empty the medium reservoirs but not the microfluidic channels. The tip of the vacuum aspirator should be placed away from the microfluidic channel inlets.
- ▲ CRITICAL** For all the immunofluorescence staining steps, adding slightly different volumes of solutions to each medium reservoir is recommended to facilitate solution exchange in the microfluidic device. All the immunofluorescence staining steps should be conducted in a humidified chamber prepared as described in Step 9 to mitigate evaporation of the medium reservoir.
- (i) At desired endpoints of assay, remove culture medium from all medium reservoirs by vacuum aspiration.
 - (ii) Add 150–200 μL 4% (wt/vol) PFA in all medium reservoirs. Leave the microfluidic device at 4 $^\circ\text{C}$ in a refrigerator overnight for cell fixation.
 - (iii) Remove PFA in all medium reservoirs by vacuum aspiration.
 - (iv) Add 200–250 μL PBS to all medium reservoirs for 10 min.
■ PAUSE POINT The microfluidic device filled with PBS can be stored at 4 $^\circ\text{C}$ in a refrigerator for 3–5 d.
 - (v) Remove PBS from all medium reservoirs by vacuum aspiration.
 - (vi) Add 150–200 μL 0.1% (vol/wt) SDS in each medium reservoir and incubate the microfluidic device for 3 h at room temperature. Then remove the SDS and wash the microfluidic device with PBS as described in Step 23B(iv and v).
 - (vii) Add 150–200 μL blocking solution to each reservoir, and incubate the microfluidic device for 24 h at 4 $^\circ\text{C}$ in a refrigerator. Remove blocking solution and wash the microfluidic device with PBS twice as described in Step 23B(iv and v).
 - (viii) Dilute primary antibodies that you wish to use for staining in blocking solution. Examples of suitable antibodies we have used and the recommended concentrations are listed in Table 1.
 - (ix) Remove blocking solution from all medium reservoirs by vacuum aspiration. Add 50–60 μL primary antibody solutions into each medium reservoir, and incubate the microfluidic device at 4 $^\circ\text{C}$ in a refrigerator for >24 h.
 - (x) Remove primary antibody solutions from all medium reservoirs by vacuum aspiration. Wash the microfluidic device with PBS twice as described in Step 23B(iv and v).
 - (xi) Prepare a working concentration of the appropriate secondary antibody (see Table 1 for details), WGA (if needed), and DAPI in blocking solution. We recommend using a dilution of 1:500 for the secondary antibody, WGA, and DAPI. Add 50–60 μL secondary antibody

solution into each medium reservoir, and incubate the microfluidic device at 4 °C in a refrigerator for 24 h. Protect the microfluidic device from light.

- (xii) Remove secondary antibody solution and wash the microfluidic device with PBS twice as described in Step 23B(iv and v). Fill the medium reservoirs with PBS.

■ PAUSE POINT The microfluidic device can be stored at 4 °C in a refrigerator for up to 2 weeks. Note that care should be taken to prevent the medium reservoirs from drying out while storing the microfluidic device.

- (xiii) Image the microfluidic device. We use a confocal microscope to take immunofluorescence images. The digital gain and exposure time are adjusted using MetaMorph Advanced. AxioVision is used to quantify the morphology of the embryonic sac-like tissues. ImageJ is used to merge color channels and generate images for publication.

? TROUBLESHOOTING

Troubleshooting

Troubleshooting advice can be found in Table 3, and see Fig. 2 for microscopy images showing examples of problems that might be encountered.

Table 3 | Troubleshooting table

Step	Problem	Possible reason	Solution
7	Defective or weak PDMS bonding	Mishandling of the bonding steps	Optimize plasma treatment power and duration Apply higher pressure for longer time when bonding on a 120 °C hotplate Wash coverslips using ethanol for a longer time
11	Geltrex leaks into the cell-loading and induction channels	Geltrex injection force is too strong Baking time of the microfluidic device at 80 °C is too short Geltrex has partially solidified before injection into the microfluidic device	Geltrex injection should be gentle Prolong baking of the microfluidic device at 80 °C Solidification of Geltrex before its injection into the microfluidic device should be avoided. Geltrex solution should always be placed on ice
12	Geltrex does not form concave pockets, or pockets are too small	Geltrex concentration is too low	Increase Geltrex concentration
18,20	Cells attach to PDMS supporting posts or the cell-loading channel	Blocking process is insufficient	mTeSR needs to be used for blocking. To do so, the medium reservoirs of the cell-loading channel should contain more mTeSR medium than the induction channel
20,22	hPSC clusters are too small	Cell seeding time is too short hPSC condition is suboptimal	Repeat Step 16 Optimize hPSC passage protocol
23	hPSC clusters become squamous amniotic cysts Geltrex becomes unstable during experiments	hPSC clusters are too small Geltrex concentration is too low Geltrex has partially solidified before injection into the microfluidic device	Increase cell seeding time Increase Geltrex concentration Solidification of Geltrex before its injection into the microfluidic device should be avoided. Geltrex solution should always be placed on ice
23B(xiii)	Weak or negative staining for specific markers	Low diffusion of antibodies within the microfluidic device	Increase antibody incubation time and/or concentration

Timing

Steps 1–7, microfluidic device fabrication: 1 d for preparation of PDMS, 0.5 d for bonding PDMS with coverslip, and 0.5 d for baking microfluidic device at 80 °C

Steps 8–14, Geltrex injection and stabilization: 2 h for Geltrex injection and 18–24 h for Geltrex stabilization

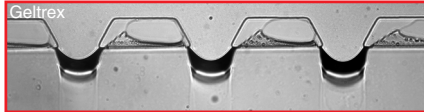
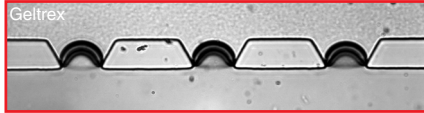
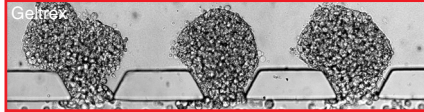
Image	Description
 <p>Gel channel</p> <p>80 μm</p>	Supporting posts are only partially bonded to the coverslip.
 <p>Geltrex</p>	Geltrex leaks into the cell-loading and/or induction channels.
 <p>Geltrex</p>	Geltrex pockets are too small.
 <p>Geltrex</p>	Cells attach to supporting posts and/or the cell-loading channel.
 <p>Geltrex</p>	Geltrex becomes unstable during experiments.
 <p>Geltrex</p> <p>$t = -18$ h</p>	hPSC clusters are too small. Small hPSC clusters will differentiate into squamous amniotic cysts when stimulated with BMP4.
 <p>Geltrex</p> <p>$t = 0$ h</p>	
 <p>Geltrex</p> <p>$t = 24$ h</p>	

Fig. 2 | Microscopy images showing examples of problems that might be encountered while implementing the protocol. These are provided to assist with troubleshooting. Scale bar, 80 μ m.

Steps 15–21, cell seeding: 0.5 h for cell dissociation and 3 h for cell seeding into the microfluidic device
 Step 22, microfluidic human embryoid generation: (i) 36 h for generation of EPI-like sacs, (ii) 36 h for generation of posteriorized or anteriorized embryonic-like sacs (A-ELS), and (iii) 48 h for generation of posteriorized or anteriorized gastrulating cells

Downstream analysis, Step 23A, retrieving cells for single-cell analysis: 30 min for washing embryonic sac-like tissues in the devices, 1–1.5 h for cell dissociation, and 30 min for preparation of cell suspension and counting

Downstream analysis, Step 23 B, immunofluorescence staining: 12 h for cell fixation, 3 h for cell permeabilization, 1 d for blocking, 1 d for primary antibody incubation, and 1 d for secondary antibody incubation

Anticipated results

By 18 h after initial cell seeding (designated as $t = 0$ h), hPSCs cluster in each gel pocket and nascent cavities are evident in many hPSC clusters. To generate pluripotent EPI-like sacs, BM is introduced into all medium reservoirs from $t = 0$ h onward. By $t = 36$ h, progressive lumenogenesis resolves loosely clustered hPSCs in each gel pocket into an expanding epithelial sac containing a single central lumen, with apical surface facing inward. The luminal surface of EPI-like sacs stains positive for EZRIN and WGA, and the lumen is enclosed by a single layer of columnar cells expressing pluripotency markers OCT4, NANOG, and SOX2 (Fig. 3a).

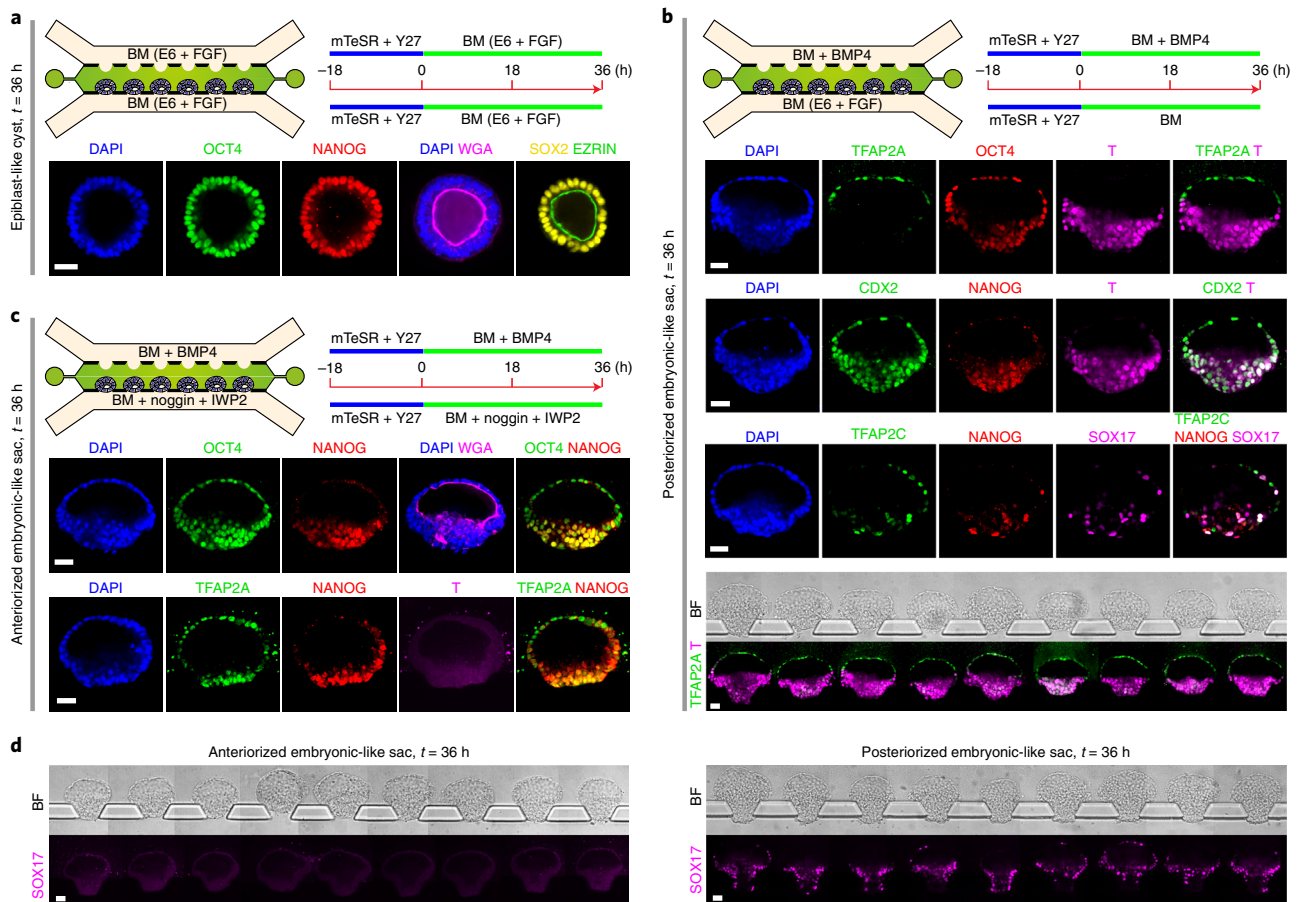


Fig. 3 | Microfluidic generations of epiblast-like cyst, posteriorized embryonic-like sac (P-ELS), and anteriorized embryonic-like sac (A-ELS). **a**, Epiblast-like (pluripotent) cyst. After initial seeding and clustering of hPSCs ($t = -18$ to 0 h), a BM comprising Essential 6 (E6) medium and FGF2 (20 ng mL^{-1}) is supplied to both the cell-loading and induction channels from $t = 0$ h onward. Representative confocal micrographs showing epiblast-like cysts at $t = 36$ h stained for OCT4, NANOG, SOX2, and EZRIN. Fluorescently labeled WGA was used to stain plasma membrane. Experiments repeated five times showed similar results. **b**, P-ELS. After initial seeding and clustering of hPSCs ($t = -18$ to 0 h), BMP4 stimulation (50 ng mL^{-1}) from the induction channel from $t = 0$ h onward leads to the formation of the asymmetric embryonic-like sac, with specification of the AM-like fate to cells directly exposed to BMP4 induction and expression of PS markers in the epiblast-like compartment. Representative confocal micrographs showing P-ELS at $t = 36$ h stained for TFAP2A, OCT4, and T; CDX2, NANOG, and T; TFAP2C, NANOG, and SOX17. Experiments repeated five times showed similar results. Bottom: Bright-field and immunostaining images showing an array of P-ELS within the same microfluidic device at $t = 36$ h, stained for TFAP2A and T. **c**, A-ELS. After initial seeding and clustering of hPSCs ($t = -18$ to 0 h), BMP4 (50 ng mL^{-1}) stimulation from $t = 0$ h onward in the induction channel leads to induction of the AM-like fate for hPSCs directly exposed to BMP4 stimulation. Inhibition of BMP and Wnt signaling by supplementing Noggin (50 ng mL^{-1}) and IWP2 ($5 \mu\text{M}$) in the cell-loading channel prevents the epiblast-like compartment from losing pluripotency and initiating gastrulation-like events. Representative confocal micrographs showing A-ELS at $t = 36$ h stained for OCT4 and NANOG; TFAP2A, NANOG, and T. Plasma membrane was stained with fluorescently labeled WGA. Experiments repeated four times showed similar results. **d**, Bright-field and immunostaining images showing an array of A-ELS (left) and P-ELS (right) at $t = 36$ h, stained for SOX17. In **a-c**, nuclei were counterstained with DAPI. Scale bars, $40 \mu\text{m}$. BM, basal medium (E6 and FGF2). The schematic of each protocol is adapted from ref. ²⁹.

To generate posteriorized embryonic-like sacs (P-ELS), BMP4 is supplemented into the induction channel from $t = 0$ h onward. Note that the cluster size of hPSCs at $t = 0$ h before supplementing exogenous factors into the cell-loading and/or induction channels is an important consideration affecting the development of human embryonic-like sacs. The hPSC cluster at $t = 0$ h needs to be large enough to occupy the entire space between adjacent supporting posts, in order to block BMP4 loaded into either the cell-loading or induction channel from reaching the opposite channel. However, the hPSC cluster at $t = 0$ h should not be so large that the cell cluster contains multiple lumens or significantly slows down the gastrulating cell induction process. It is critical that the medium reservoirs of the induction channel always contain slightly more medium than the reservoirs of the cell-loading channel, to ensure that hPSC clusters entrapped in each gel pocket are pressed against supporting posts. From $t = 0$ h onward, nascent cavities emerge in hPSC clusters. By $t = 24$ h, cells in each hPSC cluster directly exposed to BMP4 stimulation start to become squamous and flattened, reflecting their fate transition from pluripotent cells to amniotic cells. At $t = 36$ h, each hPSC cluster

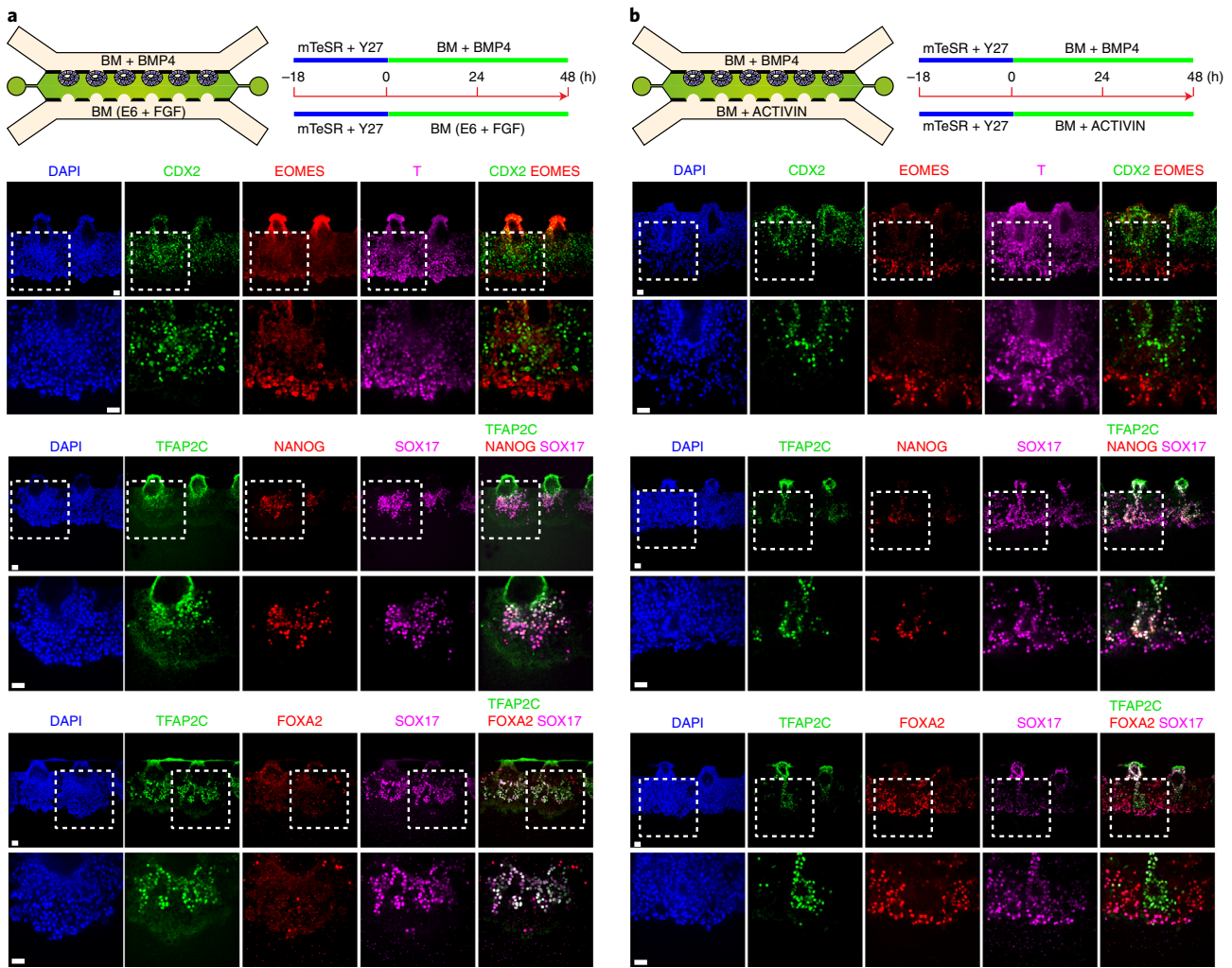


Fig. 4 | Posteriorized and anteriorized gastrulating cell development in the microfluidic device. **a**, Posteriorized gastrulating cell development. After initial seeding and clustering of hPSCs ($t = -18$ to 0 h), BMP4 stimulation (50 ng mL^{-1}) from the cell-loading channel from $t = 0$ h onward leads to the formation of the asymmetric embryonic-like sac, with specification of the AM-like fate to cells directly exposed to BMP4 induction. Cell dissemination from the EPI-like compartment was evident. Representative confocal micrographs showing P-ELS at $t = 48$ h stained for CDX2, EOMES, and T; TFAP2C, NANOG, and SOX17; TFAP2C, FOXA2, and SOX17. Outlined regions are magnified in the panel below. Experiments repeated three times showed similar results. **b**, Anteriorized gastrulating cell development. After initial seeding and clustering of hPSCs ($t = -18$ to 0 h), BMP4 (50 ng mL^{-1}) and Activin-A (50 ng mL^{-1}) were supplemented into the cell-loading and induction channels, respectively, from $t = 0$ h onward. Representative confocal micrographs at $t = 48$ h showing staining for CDX2, EOMES, and T; TFAP2C, NANOG, and SOX17; TFAP2C, FOXA2, and SOX17. Outlined regions are magnified in the panel below. Experiments repeated three times showed similar results. In all micrographs, nuclei were stained with DAPI. Scale bars, $40 \mu\text{m}$. The schematic of each protocol is adapted from ref. ²⁹.

has developed into an asymmetric sac, with a single layer of flattened, AM-like epithelium at the pole exposed to BMP4 and a stratified, EPI-like epithelium containing columnar cells at the opposite pole. TFAP2A, an AM marker, is exclusively expressed in the nuclei of the AM-like epithelium. CDX2, a marker for both AM and posterior primitive streak (PS), and brachyury (also known as T-box transcription factor or T) are positive for the cells in the EPI-like compartment. At $t = 36$ h, NANOG is only retained at the center of the EPI-like compartment. TFAP2C⁺SOX17⁺NANOG⁺ hPGC-like cells (hPGCLCs) are evident in both the AM-like and EPI-like poles (Fig. 3b).

To generate anteriorized embryonic-like sacs (A-ELS), IWP2 (a Wnt inhibitor) and Noggin (a BMP inhibitor) are supplemented into the cell-loading channel in addition to BMP4 in the induction channel from $t = 0$ h onward. At $t = 36$ h, BMP4 stimulation from the induction channel still elicits patterning to confer amniotic fate on cells directly exposed to BMP4, as evidenced by flattened morphology and positive staining for TFAP2A. At $t = 36$ h, the EPI-like pole appears more organized and expresses both OCT4 and NANOG, but not T (Fig. 3c). TFAP2C⁺SOX17⁺NANOG⁺ hPGCLCs were only detected in P-ELS but not A-ELS (Fig. 3d).

Improved efficiency is a major advantage of this microfluidic human embryoid system (with an efficiency of ~95%), compared with the Gel-3D culture. The criteria utilized for quantifying the successful generation of embryonic-like sacs include a single central lumen and immunocytochemistry to confirm molecular asymmetry (for P-ELS, co-staining for TFAP2A and T (Fig. 3b); for A-ELS, co-staining for TFAP2A and NANOG (Fig. 3c)). The main sources of variability come from the gel pocket formation and the size of hPSC clusters before supplementing exogenous factors at $t = 0$ h. A properly trained researcher can run up to 30 devices in parallel per experiment.

To generate posteriorized gastrulating cells, BMP4 is supplemented into the cell-loading channel. In this case, flattening of AM-like cells at the pole exposed to BMP4 is evident at $t = 18$ h. Cells at the opposite EPI-like pole become significantly thickened at $t = 36$ h. From $t = 36$ h onward, individual cells start emigrating from the EPI-like pole and morphologically acquire a mesenchymal phenotype. At $t = 48$ h, variable levels of T, EOMES, and CDX2 are detected in emigrating cells; leading cells are T^{high}, EOMES⁺, and CDX2⁻, whereas trailing cells, in contrast, are T^{low}, EOMES⁻, and CDX2⁺. TFAP2C⁺SOX17⁺NANOG⁺ hPGCLCs appear as cell clusters and migrate together with gastrulating cells (Fig. 4a).

To generate anteriorized gastrulating cells, from $t = 0$ h onward, Activin-A is supplemented into the induction channel, in addition to BMP4 in the cell-loading channel. Cells start disseminating from the opposite EPI-like pole at around $t = 24$ h. At $t = 48$ h, compared with the posteriorized gastrulating cell phenotype, leading cells appear more mesenchymal and are EOMES^{high}; many leading disseminating cells are SOX17⁺/FOXA2⁺, suggesting that these cells are in transition to an endoderm fate (Fig. 4b). In distinct contrast, significantly fewer leading disseminating cells are SOX17⁺/FOXA2⁺ in the posteriorized gastrulating cell protocol. Significantly fewer TFAP2C⁺SOX17⁺NANOG⁺ hPGCLCs are present in the anteriorized, compared with posteriorized, gastrulating cell protocol (Fig. 4b).

Reporting Summary

Further information on research design is available in the Nature Research Reporting Summary linked to this article.

Data availability

Representative results obtained using this protocol are available within the article, with additional examples available from the corresponding author upon request.

References

1. Koot, Y. E. M., Teklenburg, G., Salker, M. S., Brosens, J. J. & Macklon, N. S. Molecular aspects of implantation failure. *Biochim. Biophys. Acta Mol. Basis Dis* **1822**, 1943–1950 (2012).
2. Bianco-Miotto, T., Craig, J. M., Gasser, Y. P., van Dijk, S. J. & Ozanne, S. E. Epigenetics and DOHaD: from basics to birth and beyond. *J. Dev. Orig. Health Dis* **8**, 513–519 (2017).
3. Petropoulos, S. et al. Single-cell RNA-Seq reveals lineage and X chromosome dynamics in human preimplantation embryos. *Cell* **165**, 1012–1026 (2016).
4. Yan, L. et al. Single-cell RNA-Seq profiling of human preimplantation embryos and embryonic stem cells. *Nat. Struct. Mol. Biol.* **20**, 1131–1139 (2013).
5. Blakeley, P. et al. Defining the three cell lineages of the human blastocyst by single-cell RNA-Seq. *Development* **142**, 3151–3165 (2015).
6. Fogarty, N. M. E. et al. Genome editing reveals a role for OCT4 in human embryogenesis. *Nature* **550**, 67–73 (2017).
7. Hurlbut, J. B. et al. Revisiting the Warnock rule. *Nat. Biotechnol.* **35**, 1029–1042 (2017).
8. Williams, K. & Johnson, M. H. Adapting the 14-day rule for embryo research to encompass evolving technologies. *Reprod. Biomed. Soc. Online* **10**, 1–9 (2020).
9. Hyun, I., Wilkerson, A. & Johnston, J. Embryology policy: revisit the 14-day rule. *Nature* <https://doi.org/10.1038/533169a> (2016).
10. Rossant, J. & Tam, P. P. L. Exploring early human embryo development. *Science* **360**, 1075–1076 (2018).
11. Rossant, J. Mouse and human blastocyst-derived stem cells: vive les differences. *Development* **142**, 9–12 (2015).
12. Rossant, J. & Tam, P. P. L. New insights into early human development: lessons for stem cell derivation and differentiation. *Cell Stem Cell* **20**, 18–28 (2017).
13. Deglincerti, A. et al. Self-organization of the in vitro attached human embryo. *Nature* **533**, 1–13 (2016).
14. Shahbazi, M. N. et al. Self-organization of the human embryo in the absence of maternal tissues. *Nat. Cell Biol.* **18**, 700–708 (2016).

15. Ma, H. et al. In vitro culture of cynomolgus monkey embryos beyond early gastrulation. *Science* **366**, eaax7890 (2019).
16. Niu, Y. et al. Dissecting primate early post-implantation development using long-term in vitro embryo culture. *Science* **366**, eaaw5754 (2019).
17. Xiang, L. et al. A developmental landscape of 3D-cultured human pre-gastrulation embryos. *Nature* **577**, 537–542 (2019).
18. Guo, H. et al. The DNA methylation landscape of human early embryos. *Nature* **511**, 606–610 (2014).
19. Nakamura, T. et al. A developmental coordinate of pluripotency among mice, monkeys and humans. *Nature* **537**, 57–62 (2016).
20. Hackett, J. A. & Surani, M. A. Regulatory principles of pluripotency: from the ground state up. *Cell Stem Cell* **15**, 416–430 (2014).
21. Nichols, J. & Smith, A. Naive and primed pluripotent states. *Cell Stem Cell* **4**, 487–492 (2009).
22. Warmflash, A., Sorre, B., Etoc, F., Siggia, E. D. & Brivanlou, A. H. A method to recapitulate early embryonic spatial patterning in human embryonic stem cells. *Nat. Methods* **11**, 847 (2014).
23. Shao, Y. et al. Self-organized amniogenesis by human pluripotent stem cells in a biomimetic implantation-like niche. *Nat. Mater.* **16**, 419–425 (2016).
24. Shao, Y. et al. A pluripotent stem cell-based model for post-implantation human amniotic sac development. *Nat. Commun.* **8**, 208 (2017).
25. Xue, X. et al. Mechanics-guided embryonic patterning of neuroectoderm tissue from human pluripotent stem cells. *Nat. Mater.* **17**, 633–641 (2018).
26. Haremake, T. et al. Self-organizing neuruloids model developmental aspects of Huntington's disease in the ectodermal compartment. *Nat. Biotechnol.* **37**, 1198–1208 (2019).
27. Simunovic, M. et al. A 3D model of a human epiblast reveals BMP4-driven symmetry breaking. *Nat. Cell Biol.* **21**, 900–910 (2019).
28. Zheng, Y. et al. Dorsal–ventral patterned neural cyst from human pluripotent stem cells in a neurogenic niche. *Sci. Adv.* **5**, eaax5933 (2019).
29. Zheng, Y. et al. Controlled modelling of human epiblast and amnion development using stem cells. *Nature* **573**, 421–425 (2019).
30. Li, R. et al. Generation of blastocyst-like structures from mouse embryonic and adult cell cultures. *Cell* **179**, 687–702.e18 (2019).
31. Rivron, N. C. et al. Blastocyst-like structures generated solely from stem cells. *Nature* **557**, 106–111 (2018).
32. Sozen, B. et al. Self-assembly of embryonic and two extra-embryonic stem cell types into gastrulating embryo-like structures. *Nat. Cell Biol.* **20**, 979–989 (2018).
33. Harrison, S. E., Sozen, B., Christodoulou, N., Kyprianou, C. & Zernicka-Goetz, M. Assembly of embryonic and extraembryonic stem cells to mimic embryogenesis in vitro. *Science* **356**, eaal1810 (2017).
34. Beccari, L. et al. Multi-axial self-organization properties of mouse embryonic stem cells into gastruloids. *Nature* **562**, 272–276 (2018).
35. van den Brink, S. C. et al. Symmetry breaking, germ layer specification and axial organisation in aggregates of mouse embryonic stem cells. *Development* **141**, 4231–4242 (2014).
36. ten Berge, D. et al. Wnt signaling mediates self-organization and axis formation in embryoid bodies. *Cell Stem Cell* **3**, 508–518 (2008).
37. Sozen, B. et al. Self-organization of mouse stem cells into an extended potential blastoid. *Dev. Cell* **51**, 698–712.e8 (2019).
38. Tewary, M. et al. A stepwise model of reaction-diffusion and positional information governs self-organized human peri-gastrulation-like patterning. *Development* **144**, 4298–4312 (2017).
39. Taniguchi, K. et al. Lumen formation is an intrinsic property of isolated human pluripotent stem cells. *Stem Cell Rep.* **5**, 954–962 (2015).
40. Meinhardt, A. et al. 3D reconstitution of the patterned neural tube from embryonic stem cells. *Stem Cell Rep.* **3**, 987–999 (2014).
41. Shao, Y. & Fu, J. Integrated micro/nanoengineered functional biomaterials for cell mechanics and mechanobiology: a materials perspective. *Adv. Mater.* **26**, 1494–1533 (2014).
42. Sun, Y., Chen, C. S. & Fu, J. Forcing stem cells to behave: a biophysical perspective of the cellular microenvironment. *Annu. Rev. Biophys.* **41**, 519–542 (2012).
43. Mann, J. M., Lam, R. H. W., Weng, S., Sun, Y. & Fu, J. A silicone-based stretchable micropost array membrane for monitoring live-cell subcellular cytoskeletal response. *Lab Chip* **12**, 731–740 (2012).
44. Lam, R. H. W., Sun, Y., Chen, W. & Fu, J. Elastomeric microposts integrated into microfluidics for flow-mediated endothelial mechanotransduction analysis. *Lab Chip* **12**, 1865–1873 (2012).
45. Tak For Yu, Z. et al. Rapid, automated, parallel quantitative immunoassays using highly integrated microfluidics and AlphaLISA. *Sci. Rep.* **5**, 11339 (2015).
46. Yu, Z. T. F., Cheung, M. K., Liu, S. X. & Fu, J. Accelerated biofluid filling in complex microfluidic networks by vacuum-pressure accelerated movement (V-PAM). *Small* **12**, 4521–4530 (2016).
47. Linneberg-Agerholm, M. et al. Naïve human pluripotent stem cells respond to Wnt, Nodal and LIF signalling to produce expandable naïve extra-embryonic endoderm. *Development* **146**, dev180620 (2019).
48. Anderson, K. G. V. et al. Insulin fine-tunes self-renewal pathways governing naive pluripotency and extra-embryonic endoderm. *Nat. Cell Biol.* **19**, 1164–1177 (2017).

49. Fu, J., Mao, P. & Han, J. Continuous-flow bioseparation using microfabricated anisotropic nanofluidic sieving structures. *Nat. Protoc.* **4**, 1681–1698 (2009).
50. Yang, M. T., Fu, J., Wang, Y., Desai, R. A. & Chen, C. S. Assaying stem cell mechanobiology on micro-fabricated elastomeric substrates with geometrically modulated rigidity. *Nat. Protoc.* **6**, 187–213 (2011).
51. Shin, Y. et al. Microfluidic assay for simultaneous culture of multiple cell types on surfaces or within hydrogels. *Nat. Protoc.* **7**, 1247–1259 (2012).
52. Chen, H. M. et al. Transcripts involved in calcium signaling and telencephalic neuronal fate are altered in induced pluripotent stem cells from bipolar disorder patients. *Transl. Psychiatry* **4**, e375–e375 (2014).
53. Daley, G. Q. et al. Setting global standards for stem cell research and clinical translation: the 2016 ISSCR guidelines. *Stem Cell Rep.* **6**, 787–797 (2016).
54. Rivron, N. et al. Debate ethics of embryo models from stem cells. *Nature* **564**, 183–185 (2018).
55. Satija, R., Farrell, J. A., Gennert, D., Schier, A. F. & Regev, A. Spatial reconstruction of single-cell gene expression data. *Nat. Biotechnol.* **33**, 495–502 (2015).
56. Butler, A., Hoffman, P., Smibert, P., Papalexi, E. & Satija, R. Integrating single-cell transcriptomic data across different conditions, technologies, and species. *Nat. Biotechnol.* **36**, 411–420 (2018).

Acknowledgements

This work is supported by the University of Michigan Mechanical Engineering Faculty Support Fund, the Michigan-Cambridge Research Initiative, and the University of Michigan Mcubed Fund. The Lurie Nanofabrication Facility at the University of Michigan is acknowledged for support with microfabrication.

Author contributions

Y.Z. and J.F. conceived and initiated the project; Y.Z. designed, performed, and quantified the experiments; Y.S. helped to design experiments; Y.Z. and J.F. wrote the manuscript; J.F. supervised the study. All authors edited and approved the manuscript.

Competing interests

Y.Z., Y.S., and J.F. have filed two provisional patents related to this work (US provisional patent application nos. 62/431,907 and 62/897,565).

Additional information

Supplementary information is available for this paper at <https://doi.org/10.1038/s41596-020-00417-w>.

Correspondence and requests for materials should be addressed to J.F.

Peer review information *Nature Protocols* thanks Guohao Dai, Eric Siggia, and Patrick Tam for their contribution to the peer review of this work.

Reprints and permissions information is available at www.nature.com/reprints.

Publisher's note Springer Nature remains neutral with regard to jurisdictional claims in published maps and institutional affiliations.

Received: 1 April 2020; Accepted: 22 September 2020;

Published online: 11 December 2020

Related links

Key references using this protocol

Zheng, Y. et al. *Nature* **573**, 421–425 (2019): <https://doi.org/10.1038/s41586-019-1535-2>

Shao, Y. et al. *Nat. Mater.* **16**, 419–425 (2017): <https://doi.org/10.1038/nmat4829>

Shao, Y. et al. *Nat. Commun.* **8**, 208 (2017): <https://doi.org/10.1038/s41467-017-00236-w>

Reporting Summary

Nature Research wishes to improve the reproducibility of the work that we publish. This form provides structure for consistency and transparency in reporting. For further information on Nature Research policies, see our [Editorial Policies](#) and the [Editorial Policy Checklist](#).

Statistics

For all statistical analyses, confirm that the following items are present in the figure legend, table legend, main text, or Methods section.

n/a Confirmed

- | | | |
|-------------------------------------|-------------------------------------|------------------------------------------------------------------------------------------------------------------------------------------------------------------------------------------------------------------------------------------------------------|
| <input type="checkbox"/> | <input checked="" type="checkbox"/> | The exact sample size (n) for each experimental group/condition, given as a discrete number and unit of measurement |
| <input type="checkbox"/> | <input checked="" type="checkbox"/> | A statement on whether measurements were taken from distinct samples or whether the same sample was measured repeatedly |
| <input checked="" type="checkbox"/> | <input type="checkbox"/> | The statistical test(s) used AND whether they are one- or two-sided
<i>Only common tests should be described solely by name; describe more complex techniques in the Methods section.</i> |
| <input type="checkbox"/> | <input checked="" type="checkbox"/> | A description of all covariates tested |
| <input checked="" type="checkbox"/> | <input type="checkbox"/> | A description of any assumptions or corrections, such as tests of normality and adjustment for multiple comparisons |
| <input checked="" type="checkbox"/> | <input type="checkbox"/> | A full description of the statistical parameters including central tendency (e.g. means) or other basic estimates (e.g. regression coefficient) AND variation (e.g. standard deviation) or associated estimates of uncertainty (e.g. confidence intervals) |
| <input checked="" type="checkbox"/> | <input type="checkbox"/> | For null hypothesis testing, the test statistic (e.g. F , t , r) with confidence intervals, effect sizes, degrees of freedom and P value noted
<i>Give P values as exact values whenever suitable.</i> |
| <input checked="" type="checkbox"/> | <input type="checkbox"/> | For Bayesian analysis, information on the choice of priors and Markov chain Monte Carlo settings |
| <input checked="" type="checkbox"/> | <input type="checkbox"/> | For hierarchical and complex designs, identification of the appropriate level for tests and full reporting of outcomes |
| <input checked="" type="checkbox"/> | <input type="checkbox"/> | Estimates of effect sizes (e.g. Cohen's d , Pearson's r), indicating how they were calculated |

Our web collection on [statistics for biologists](#) contains articles on many of the points above.

Software and code

Policy information about [availability of computer code](#)

Data collection

Data analysis

For manuscripts utilizing custom algorithms or software that are central to the research but not yet described in published literature, software must be made available to editors and reviewers. We strongly encourage code deposition in a community repository (e.g. GitHub). See the Nature Research [guidelines for submitting code & software](#) for further information.

Data

Policy information about [availability of data](#)

All manuscripts must include a [data availability statement](#). This statement should provide the following information, where applicable:

- Accession codes, unique identifiers, or web links for publicly available datasets
- A list of figures that have associated raw data
- A description of any restrictions on data availability

Data supporting the findings of this study are available within the article and its supplementary information files and from the corresponding authors upon reasonable request.

Field-specific reporting

Please select the one below that is the best fit for your research. If you are not sure, read the appropriate sections before making your selection.

Life sciences Behavioural & social sciences Ecological, evolutionary & environmental sciences

For a reference copy of the document with all sections, see [nature.com/documents/nr-reporting-summary-flat.pdf](https://www.nature.com/documents/nr-reporting-summary-flat.pdf)

Life sciences study design

All studies must disclose on these points even when the disclosure is negative.

Sample size	All experiments were conducted with at least two independent experiments and multiple biological replicates. Sample sizes were determined based on our previous experience and similar studies of other groups. Sample sizes were determined as sufficient since they led to similar results.
Data exclusions	Due to intrinsic inhomogeneity of Geltrex, some Geltrex continued to contract during experiments. Such experiments were excluded from data analysis. In rare cases, after initial cell seeding, concave Geltrex pockets between neighboring supporting posts could be damaged. Cell clusters formed within such damaged gel pockets were excluded from data analysis. No similar platform has been previously reported, thus the criteria were established specifically for this platform.
Replication	Reported results were repeated and confirmed for at least two independent experiments. Key experimental findings were reliably reproduced by two investigators involved in this work.
Randomization	Samples were randomly allocated to control and different experimental groups (see Methods). However, no particular randomization method was used in this work.
Blinding	Investigators were not blinded to group allocation, as no animal/human studies were conducted in this manuscript.

Reporting for specific materials, systems and methods

We require information from authors about some types of materials, experimental systems and methods used in many studies. Here, indicate whether each material, system or method listed is relevant to your study. If you are not sure if a list item applies to your research, read the appropriate section before selecting a response.

Materials & experimental systems

n/a	Involved in the study
<input type="checkbox"/>	<input checked="" type="checkbox"/> Antibodies
<input type="checkbox"/>	<input checked="" type="checkbox"/> Eukaryotic cell lines
<input checked="" type="checkbox"/>	<input type="checkbox"/> Palaeontology and archaeology
<input checked="" type="checkbox"/>	<input type="checkbox"/> Animals and other organisms
<input checked="" type="checkbox"/>	<input type="checkbox"/> Human research participants
<input checked="" type="checkbox"/>	<input type="checkbox"/> Clinical data
<input checked="" type="checkbox"/>	<input type="checkbox"/> Dual use research of concern

Methods

n/a	Involved in the study
<input checked="" type="checkbox"/>	<input type="checkbox"/> ChIP-seq
<input checked="" type="checkbox"/>	<input type="checkbox"/> Flow cytometry
<input checked="" type="checkbox"/>	<input type="checkbox"/> MRI-based neuroimaging

Antibodies

Antibodies used

Only certified and company-validated antibodies were used in this work:

Primary antibodies:

EZRIN Sigma-Aldrich Cat# E8897, RRID:AB_476955 Mouse 1:200
 OCT4 Santa Cruz Biotechnology Cat# sc-5279, RRID:AB_628051 Mouse 1:200
 OCT4 Cell Signaling Technology Cat# 2750, RRID:AB_823583 Rabbit 1:500
 NANOG Cell Signaling Technology Cat# 4903, RRID:AB_10559205 Rabbit 1:500
 SOX2 Stemgent Cat# 09-0024, RRID:AB_2195775 Rabbit 1:500
 TFAP2A Santa Cruz Biotechnology Cat# sc-12726, RRID:AB_667767 Mouse 1:100
 TFAP2C Santa Cruz Biotechnology Cat# sc-12762, RRID:AB_667770 Mouse 1:100
 BRACHYURY Thermo Fisher Scientific Cat# PA5-46984, RRID:AB_2610378 Goat 1:100
 SOX17 R and D Systems Cat# AF1924, RRID:AB_355060 Goat 1:500
 CDX2 BioGenex Cat# AM392, RRID:AB_2650531 Mouse 1:300
 FOXA2 Cell Signaling Technology Cat# 8186, RRID:AB_10891055 Rabbit 1:300
 EOMES Abcam Cat# ab23345, RRID:AB_778267 Rabbit 1:200

Secondary antibodies:

Donkey anti-Rabbit 546 Thermo Fisher Scientific Cat# A10040, RRID:AB_2534016 1:500

Donkey anti-Mouse 488 Thermo Fisher Scientific Cat# A-21202, RRID:AB_141607 1:500
Donkey anti-Goat 647 Thermo Fisher Scientific Cat# A-21447, RRID:AB_2535864 1:500

The antibody information (including species, application, and catalog number) has been provided in Supplementary Information.

Validation

All antibodies have been validated by the companies from which they were purchased. The subcellular localization of all the proteins analyzed in this work is consistent with previous published literatures. This information was used to further validate the specificity. Details about validation statements of the manufacturer, relevant citations and antibody profiles can be found on the manufacturer's website.

Eukaryotic cell lines

Policy information about [cell lines](#)

Cell line source(s)

The following cell lines were used in this work:
H9 hESC line (WA09, WiCell; NIH registration number: 0062); H1 hESC line (WA01, WiCell; NIH registration number: 0043); A hiPSC line (1196a) originally reported in Villa-Diaz, L. G. et al. Nat. Biotechnol. 28, 581 (2010).

Authentication

All hPSC lines have been authenticated by the original sources and also authenticated in-house by immunostaining for pluripotency markers and successful differentiation to the three germ layer cells.

Mycoplasma contamination

All cell lines used in this work have been tested negative for mycoplasma contamination.

Commonly misidentified lines (See [ICLAC](#) register)

No commonly misidentified cell lines listed by ICLAC were used in this work.